EXPERIMENTAL STUDIES OF RESONANCE CROSSING IN LINEAR NON-SCALING FFAGS WITH THE S-POD PLASMA TRAP

S. L. Sheehy*, D. J. Kelliher, S. Machida, C. R. Prior, ASTeC/RAL/STFC, Oxon, UK
K. Fukushima, K. Ito, K. Moriya, T. Okano, H. Okamoto, University of Hiroshima, Japan

Abstract

In a linear non-scaling FFAG the betatron tunes vary over a wide range during acceleration. This naturally leads to multiple resonance crossing including first order integer resonances. The S-POD (Simulator for Particle Orbit Dynamics) plasma trap apparatus at Hiroshima University represents a physically equivalent system to a charged particle beam travelling in a strong focusing accelerator lattice. The S-POD system can be used as an experimental simulation to investigate the effects of resonance crossing and its dependence on dipole errors, tune crossing speed and other factors. Recent developments and experiments are discussed.

INTRODUCTION

Linear non-scaling fixed field alternating gradient accelerators (ns-FFAGs) have naturally large negative uncorrected chromaticity, so the betatron tunes cross many integer and half-integer resonances during acceleration. If resonance crossing is sufficiently fast and the error driving terms are small, it is expected that the betatron amplitudes should not grow, *ie.* the resonance will be crossed without considerable deterioration of the beam.

The electron model ns-FFAG 'EMMA' completes acceleration in less than 10 turns. EMMA is able to successfully operate while crossing multiple integer resonances [1]. Work is ongoing to study the slow resonance crossing regime experimentally using EMMA [2]. However, it is observed that EMMA has a large closed orbit distortion which is thought to arise from stray magnetic field from the injection septum. Such a dipole term will naturally drive integer resonances in the machine and thus limit the scope of the slow crossing studies.

Other ns-FFAG designs naturally have much slower resonance crossing rates. For example some designs for proton therapy [3] have a much slower acceleration rate and would thus have a slower tune slew rate which is expected to be detrimental [4, 5]. Concerns about beam deterioration due to resonance crossing has led to proton ns-FFAG designs which avoid resonance crossing through the introduction of higher order multipole fields and field shaping [6, 7, 8].

These applications motivate us to understand the phenomenon of resonance crossing in ns-FFAGs for various crossing speeds and driving terms, to ascertain whether proposed models of resonance crossing such as Baartman's [9, 10] hold and if so, in what parameter range.

* suzie.sheehy@stfc.ac.uk

EMMA AND S-POD CORRESPONDENCE

In order to study the effects of integer resonance crossing in a controlled environment, we rely on the isomorphism between non-neutral plasmas in a linear Paul trap and charged particle beams in a linear alternating gradient accelerator [11]. The setup known as 'S-POD' based at Hiroshima University provides an experimental apparatus to investigate detailed resonance crossing effects which may provide valuable insight into the dynamics of non-scaling FFAG accelerators. Previous work has focused on space charge driven resonances [13] whereas this work focuses on the regime with low ion number in the trap to mimic a low intensity accelerator.

In the S-POD trap the frequency of the confinement wave is 1 MHz and so the wavelength is much greater than the trap dimension. The static field approximation can then be used and the non-relativistic motion of a charged particle (mass m and charge state q) obeys the Hamiltonian:

$$H = \frac{p_x^2 + p_y^2}{2} + \frac{q}{mc^2}\phi \tag{1}$$

Simultaneously applying rf dipole and quadrupole fields and concentrating on only the x-motion (neglecting the vertical motion) the equation of motion is:

$$\frac{d^2\tilde{x}}{d\Psi^2} + \nu_0^2\tilde{x} = -(\nu_0\beta_{rf})^{3/2}D, \tag{2}$$

where the spatial co-ordinate x has been scaled and D is defined as in Eq. 3. The phase advance Ψ of the betatron oscillation β_{rf} is evaluated from Eq. 4.

$$\tilde{x} = \frac{x}{\sqrt{\nu_0\beta_{rf}}}, D = \frac{q}{mc^2 r_0}V_D \tag{3}$$

$$\Psi = \frac{1}{\nu_0}\int^{\tau}\frac{d\tau}{\beta_{rf}} \tag{4}$$

In a storage ring the equation of motion [12] is

$$\frac{d^2X_{COD}}{d\Psi^2} + \nu_0^2 X_{COD} = -(\nu_0\beta)^{3/2}\frac{\Delta B}{B\rho}, \tag{5}$$

where 'COD' means closed orbit distortion, $X_{COD} = \bar{x}_{COD}/\sqrt{\nu_0\beta}$ and β is the betatron motion. By comparing Eq. 2 and Eq. 5 we find the correspondence between the EMMA dipole perturbation field (ΔB) and the applied voltage in the S-POD setup (V_D) to be

$$V_D \approx \frac{mc^2 r_0}{q}\left(\frac{2\pi R}{N_{cell}\lambda}\right)^2\frac{\Delta B}{B\rho}, \tag{6}$$

ISBN 978-3-95450-122-9

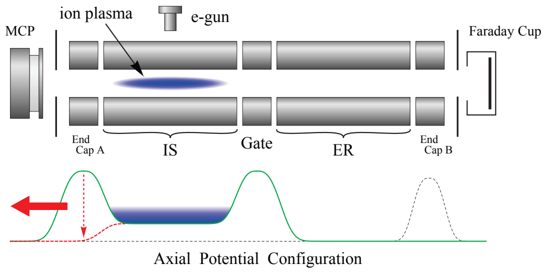

Figure 1: Schematic layout of the linear Paul trap with the confinement potential configuration.

where N_{cell} is the number of doublet cells, λ is the rf wavelength, $B\rho$ is the magnetic rigidity and the averaged value of β in a storage ring is roughly given by $\bar{\beta} = R/\nu_0$ where R is the average radius and ν_0 the tune.

S-POD Experimental Setup

The S-POD system is mainly composed of a linear Paul trap 20 cm long with a 1 cm diameter aperture housed in a vacuum vessel, supplied with DC and AC power sources. The longitudinal confinement of the ions in the trap is achieved by DC potentials on electrodes at either end of the trap shown schematically in Fig. 1 and the transverse confinement is due to an rf quadrupole field.

The $^{40}Ar^{+}$ ions are produced through electron bombardment and the plasma density is controlled by changing the neutral gas pressure and electron beam current as described in [13]. During experimental operation the ions are first confined, then the rf amplitude is selected depending on the required betatron tune. Tune variation is achieved by linearly ramping the rf voltage at a given speed. Once the ramping is completed the DC potential barrier is dropped on one side of the trap and the ions are transported towards either a faraday cup or micro channel plate (MCP) detector. The ion losses give a measure of the beam deterioration as any large amplitude ions are lost at the edges of the trap aperture.

Both quadrupolar (focusing) fields and dipole (perturbative) fields can be applied by exciting the rods in the relevant configuration, shown in Fig. 2.

EXPERIMENTAL RESULTS

Dipole Stopbands

Before completing resonance crossing experiments, the dipole stopbands are experimentally determined. The main focusing waveform is shown in Fig. 3. It mimics the case of a dipole perturbation in EMMA whose periodicity is 42. Note that the dipole pulse is actually slightly trapezoidal, not a perfect square pulse. The successful excitation of all integer resonances using this dipole pulse has been demonstrated, shown in Fig. 4. Note that due to alignment errors of the trap itself there is a large third order resonance at $3\nu_0 = 42$, a smaller fourth order resonance at $4\nu_0 = 42$ and a sixth order just visible at $6\nu_0 = 42$.

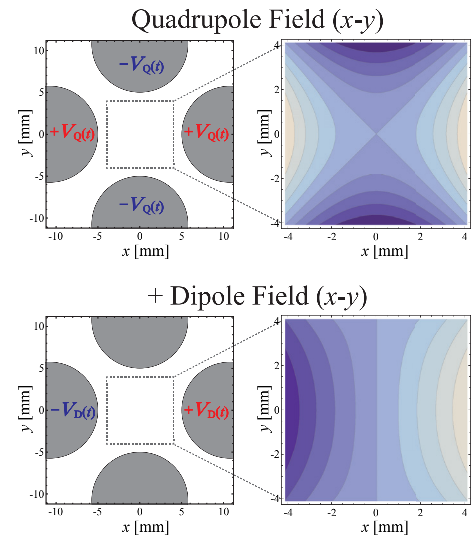

Figure 2: Schematic layout of the S-POD rods and the creation of quadrupole (focusing) and dipole (perturbative) electric fields.

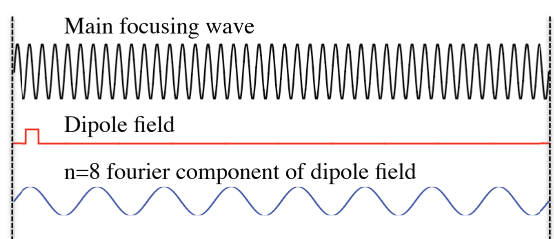

Figure 3: Schematic of the dipole pulse perturbation (red) and the n=8 fourier harmonic (blue) of the pulse together with the main focusing waveform (black).

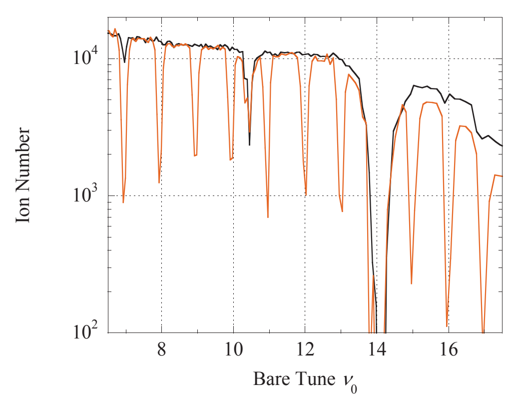

Figure 4: Experimental excitation of integer stopbands (red) using the dipole perturbation (black) without dipole perturbation.

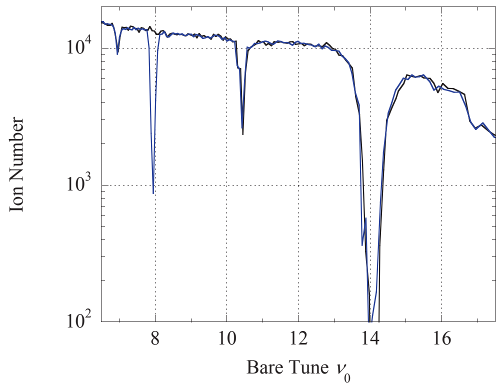

Figure 5: Excitation of the dipole stopband at one integer (blue) with control over fourier harmonics. The spectrum without dipole perturbation is shown in black.

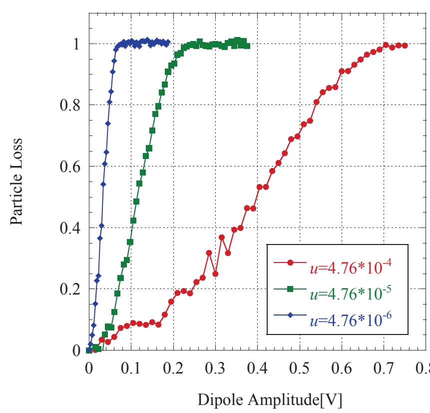

Figure 6: Single resonance crossing of the $\nu_0 = 12$ integer resonance for varying dipole amplitude at various crossing speeds.

A dipole pulse can be deconstructed into a fourier series of component perturbation waves, each of which may excite a different integer resonance. If the n=8 component (for example) is taken in isolation and applied, only the 8th integer resonance is excited. This has also been experimentally verified, as in Fig. 5.

Resonance Crossing Results

After establishing the dipole stopbands, we study single and multiple integer resonance crossing at various crossing speeds, where the crossing speed is a function of rf period (equivalent to cells) $u = \delta\nu/n_{rf}$. The single resonance crossing case is shown in Fig. 6

In the multiple crossing case we are also forced to cross the large stopbands induced by mechanical alignment issues in the trap. This means that even with zero perturbation field applied there is ion loss in the slow resonance crossing case. However, as shown in Fig. 7 it is possible to observe that at a slower crossing speed there is more particle loss.

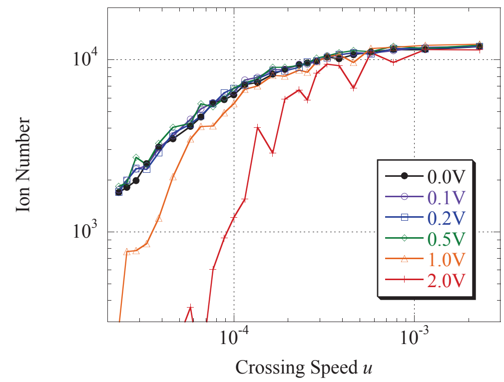

Figure 7: Multiple resonance crossing of the whole EMMA tune range for varied dipole amplitude at various crossing speeds.

FUTURE WORK

These results presented here are preliminary. In the near future we plan to study integer resonance crossing using the S-POD apparatus in more detail including single and multiple resonances, and the slow crossing regime of proton ns-FFAGs. Detailed analysis will follow.

ACKNOWLEDGMENT

This work was supported in part by a Grant-in-Aid for Scientific Research, Japan Society for the Promotion of Science.

REFERENCES

[1] S. Machida et al., Nature Physics 8, 243-247, (2012).

[2] J. Garland, IPAC'12, New Orleans, USA, p. 412, `http://www.JACoW.org`

[3] E. Keil, A. M. Sessler and D. Trbojevic, Phys. Rev. ST Accel. Beams 10, 054701 (2007).

[4] S. Machida, Phys. Rev. ST Accel. Beams 11, 094003, (2008).

[5] S. L. Sheehy and D. J. Kelliher, Int. J. Mod. Phys. 26, 1842, (2011).

[6] S. Machida, `http://www.cockcroft.ac.uk/events/FFAG08` 2008.

[7] C. Johnstone et al., PAC'09, Vancouver, BC, Canada, p. 1478, `http://www.JACoW.org`

[8] S. L. Sheehy et al., Phys. Rev. ST AB 13, 040101, (2010).

[9] R. Baartman, `http://www.triumf.ca/ffag2004/`, 2004.

[10] S. Koscielniak, R. Baartman, PAC'05, Knoxville, Tennessee, USA, p. 3206, `http://www.JACoW.org`

[11] H. Okamoto, H. Tanaka, Nucl. Instrum. Meth. A 437, 178 (1999).

[12] H. Okamoto, S. Machida, Nucl. Instrum. Meth. A, 482, 65 (2002).

[13] H. Takeuchi, et al., Phys. Rev. ST Accel. Beams 15, 174201 (2012).